3D-computed tomography to compare the dimensions of the left atrial appendage in patients with normal sinus rhythm and those with paroxysmal atrial fibrillation

Maiko Hozawa 1
Yoshihiro Morino 1✉ Phone81-19-651-5111 Emailymorino@iwate-med.ac.jp
Yuki Matsumoto 1
Ryoichi Tanaka 2
Kyohei Nagata 1
Akiko Kumagai 3
Atsushi Tashiro 4
Akio Doi 5
Kunihiro Yoshioka 2
1Division of Cardiology, Department of Internal MedicineIwate Medical University19-1 UchimaruMoriokaIwate020-8505Japan
2Department of RadiologyIwate Medical UniversityMoriokaIwateJapan
3Division of Cardioangiology, Nephrology and Endocrinology, Department of Internal MedicineIwate Medical UniversityMoriokaIwateJapan
4Division of Cardioangiology, Nephrology and Endocrinology, Department of Laboratory MedicineIwate Medical UniversityMoriokaIwateJapan
5Faculty of Software and Information ScienceIwate Prefectural UniversityMoriokaIwateJapan
Received: 25 September 2017 / Accepted: 5 January 2018

Abstract

Although paroxysmal atrial fibrillation (PAF) is an important cause of cardioembolic stroke, in contrast to chronic AF patients, the anatomical features of the left atrial appendage (LAA) in PAF patients remain unknown. Here, we investigated differences in LAA structures in patients with PAF and those with normal sinus rhythms (NSR) using 3D-computed tomography (3D-CT), which allows us to visualize complicated LAA structures at high spatial resolution. Study subjects were 30 consecutive PAF and 30 NSR patients with complete enhanced cardiac 3D-CT images available. After reconstruction of 3D LAA images, anatomical parameters of the LAA were measured and compared according to three proposed definitions of the LAA orifice plane determined by the following anatomical landmarks: DEF#1, center of warfarin ridge and centerline of proximal left circumflex artery; DEF#2, slope of warfarin ridge and mitral valve annulus; DEF#3, observers' discretion by progressive rotation using the observers' best estimate without the use of landmarks. The LAA volumes of the PAF groups were significantly greater than the NSR group according to all 3 definitions (DEF#1: 1.43 times, DEF#2: 1.44 times, and DEF#3: 1.36 times greater). The LAA orifice area was significantly larger in PAF than in NSR according to DEF#2, but was similar by DEF#1 and DEF#3. Intra-observer and inter-observer variations for any LAA measurements were very low. In conclusion, 3D-CT-based quantitative assessment of the LAA provides highly reproducible and detailed measurements, which can successfully discriminate differences of LAA volume between patients with NSR and those with PAF, suggesting significantly greater volumes in the latter.

Keywords
Left atrial appendage
Cardioembolic stroke
Paroxysmal atrial fibrillation
Orifice
Computed tomography

Introduction

Because patients with atrial fibrillation (AF) are at risk for cardioembolic stroke (CES) regardless of persistency [1], stratification of risk factors is crucially important at the initial stages of AF, as represented by paroxysmal AF (PAF). The thrombi in 90% of such patients are located in the left atrial appendage (LAA), suggesting the usefulness of a detailed evaluation of the anatomy and function of the LAA. Several transesophageal echocardiography (TEE) studies have reported a negative correlation between LAA flow velocity and prevalence of thrombus formation in the LAA [23]. On the other hand, investigations focusing on the anatomy of the LAA remain limited, especially in PAF patients. A previous study reported a positive relationship between enlargement of LAA volume and stroke event rates, suggesting that LAA size also represents a predictive factor similar to the CHADS2 or CHADS-VASC score [4]. However, such clinical investigations have mostly targeted chronic AF, and several small studies using two-dimensional (2D)- or 3D-TEE have failed to find any statistically significant differences in anatomical parameters of the LAA in patients with PAF and subjects with a normal sinus rhythm (NSR) [56]. Three-dimensional cardiac computed tomography (CT) is superior to TEE for the visualization and quantitative assessment of the LAA. We hypothesized that it may be able to discriminate small but significant differences in the LAA of patients with NSR and those with PAF. Furthermore, a precise evaluation of the LAA is becoming increasingly important because treatment using occlusion devices has now started to be applied to such patients. Three-dimensional CT assessment should be useful for such treatment planning. Accordingly, the present study sought (1) differences in the size of the LAA in subjects with an NSR and PAF patients using 3D-CT and (2) feasibility and reproducibility of 3D-CT-based quantitative assessment of the LAA.

Methods

Study population

We retrospectively surveyed a CT database library at Iwate Medical University to identify a series of examinations suitable for 3D reconstruction of the LAA, which requires the following conditions: (1) thin slice scanning for detailed 3D reconstruction, (2) sufficient contrast agent filling into the whole of the LAA, and (3) images acquired for both NSR and PAF at the identical cardiac cycle (because of contraction) [6]. A series of coronary CT angiographies satisfying these conditions was identified for the NSR subjects; the CT images targeting the left atrium that are routinely performed prior to catheter ablation were appropriate for the PAF patients. PAF was defined as atrial fibrillation within a period of 7 days and with a history of intermittent atrial fibrillation detected by electrocardiography (ECG) or Holter ECG. Patients with moderate/severe mitral valve disease, moderate/severe aortic valve disease, post-surgery mitral valve issues, left ventricular dysfunction (LVEF < 45%), dilated cardiomyopathy, hypertrophic cardiomyopathy, or chronic heart failure were excluded. A total of 30 consecutive

subjects with NSR and 30 patients with PAF was selected from this database between September 2015 and November 2016 and enrolled in this study.

Computed tomography image acquisition

For coronary CT angiography of the NSR subjects, images were acquired using a 320-detector row CT scanner (Aquilion ONE, Toshiba Medical Systems, Otawara, Japan) during injection of iopamidol (370 mg I/ml, Bayer Yakuhin, Japan) at 3.0–6.0 ml/s over 10 s using a bolus tracking technique with a threshold of 150 Hounsfield units (HU) in the ascending aorta. CT scans were performed with 0.5 mm collimation and were reconstructed at diastolic phase (near the 75% R–R interval) on the electrocardiographic gate, with a tube current of 100–450 mA [depending on body mass index (BMI)], and tube voltage of 120 kV. For LAA imaging of PAF patients, all scans were either on a 320-detector row CT scanner (Aquilion ONE, Toshiba Medical Systems, Otawara, Japan) or an 80-row helical scanner (Aquilion PRIME, Toshiba Medical Systems, Otawara, Japan) with electrocardiographic gating from the cardiac apex to the carina of the trachea at 0.5 mm collimation and 0.275 s gantry rotation. Tube current, tube voltage, and pitch factor were 100–450 mA (depending on BMI), 120 kV, and 0.145, respectively. The amount of radiation exposure from a CT examination depends on the physical build of the individual patient and the type of imaging procedure. Each CT examination was performed following the diagnostic reference level (DRL) guidelines of the J-RIME (http://www.radher.jp/J-RIME/) group. Contrast medium injection was via the right antecubital vein using iohexol (350 mg I/ml, Daiichi Sankyo Company, Japan) or iopamidol (370 mg I/ml, Bayer Yakuhin, Japan) at 3.0–6.0 ml/s over 10 s, followed by a 30 ml saline flush. Acquired data were reconstructed into 0.5 mm thickness slices at every 5% from 0 to 95% of the R–R interval. To compare with the NSR group, the phase around the 75% R–R interval was used for this analysis.

Three-dimensional reconstruction of the LAA and quantitative measurements

Off-line image analyses were performed using the commercially available software package Volume Extractor version 4.0 (i-Plants System Corporation, Morioka, Japan), which implements the functions of 3D-image processing, image editing, quantitative analyses, and 3D-model printing. This software has been widely used for pre-operative treatment planning in other medical fields such as dentistry and orthopedics [7]. Three-dimensional reconstruction of the LAA was performed using this software. This software can indicate the HU histogram for all CT slices, focuses on the threshold of contrast agent, and automatically reconstructs 3D images. This function is based on Volume Rendering. After 3D-reconstruction, quantitative measurements were performed targeting the LAA orifice and LAA volume for each patient. LAA orifice parameters included maximum diameter, minimum diameter, orifice area, and orifice symmetry (minimum diameter divided by maximum diameter). The LAA volume could be automatically calculated using this software (Fig. 1). To minimize the effects of different body size, LAA volume index was calculated as LAA volume divided by BMI. The representative LAA quantitative parameters were measured and compared between the NSR and PAF groups.

Fig. 1

Schematic of the 3D-reconstruction and segmentation of the LAA (left panel) and quantitative measurements of the orifice plane and volume of the LAA (right panels) using a commercially available software package

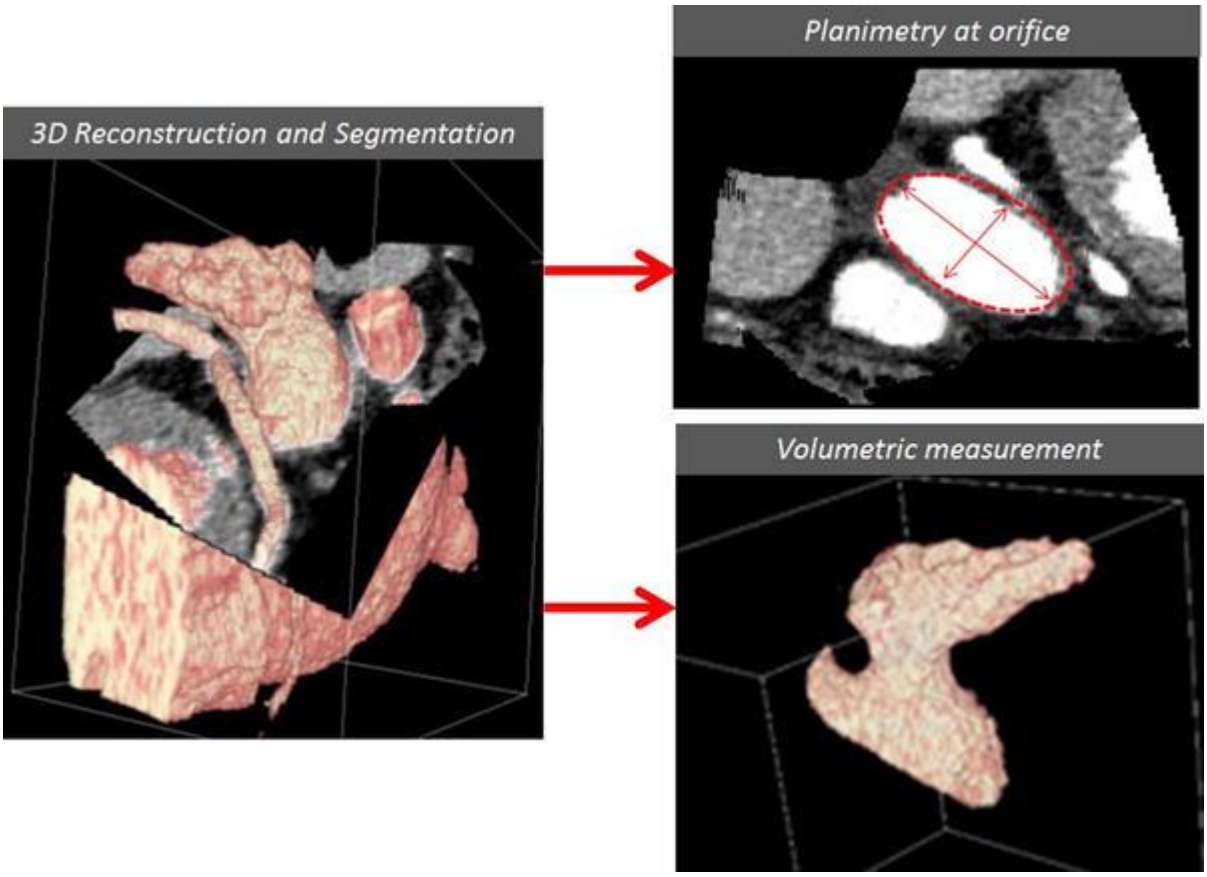

Definition of the LAA orifice plane

Three potential LAA orifice planes are possible according to the anatomical landmarks, resulting in different dimensions for measurement. Definition of the LAA plane is very important for further analyses. Basically, two points define a line, and three points define a plane. Thus, to determine the plane, either 3 arbitrary points or one line plus one point is required. Evident anatomical landmarks around the LAA orifice include the warfarin ridge, left circumflex artery (LCx) and mitral valve annulus; by combining these, three types of potential orifice plane were defined, illustrated in Fig. 2. First, definition 1 (DEF#1) was taken as the plane determined by a combination of the center of the warfarin ridge and the centerline of LCx proximal, which has generally been used with transesophageal echocardiography (TEE) [89]. Similarly, DEF#2 was defined as the plane determined by the slope of the warfarin ridge and mitral valve annulus, which has been considered as an alternative method during TEE measurements [81011]. On the other hand, DEF#3 was based on the observers' discretion by progressive rotation of LAA geometry using the observers' best estimate without the use of landmarks; this frequently corresponded to either the right anterior oblique view (RAO) caudal view or the RAO cranial view, which are commonly used during LAA implantation procedures [1011]. All the anatomical parameters of the LAA were measured for each definition separately and compared.

Fig. 2

Depictions of the three definitions of potential LAA orifice planes. DEF#1, the plane determined by the center of the warfarin ridge and the centerline of left circumflex artery proximal; DEF#2, the plane determined by the slope of the warfarin ridge and mitral valve annulus; DEF#3, the plane established at the observer's discretion by progressive rotation of LAA geometry

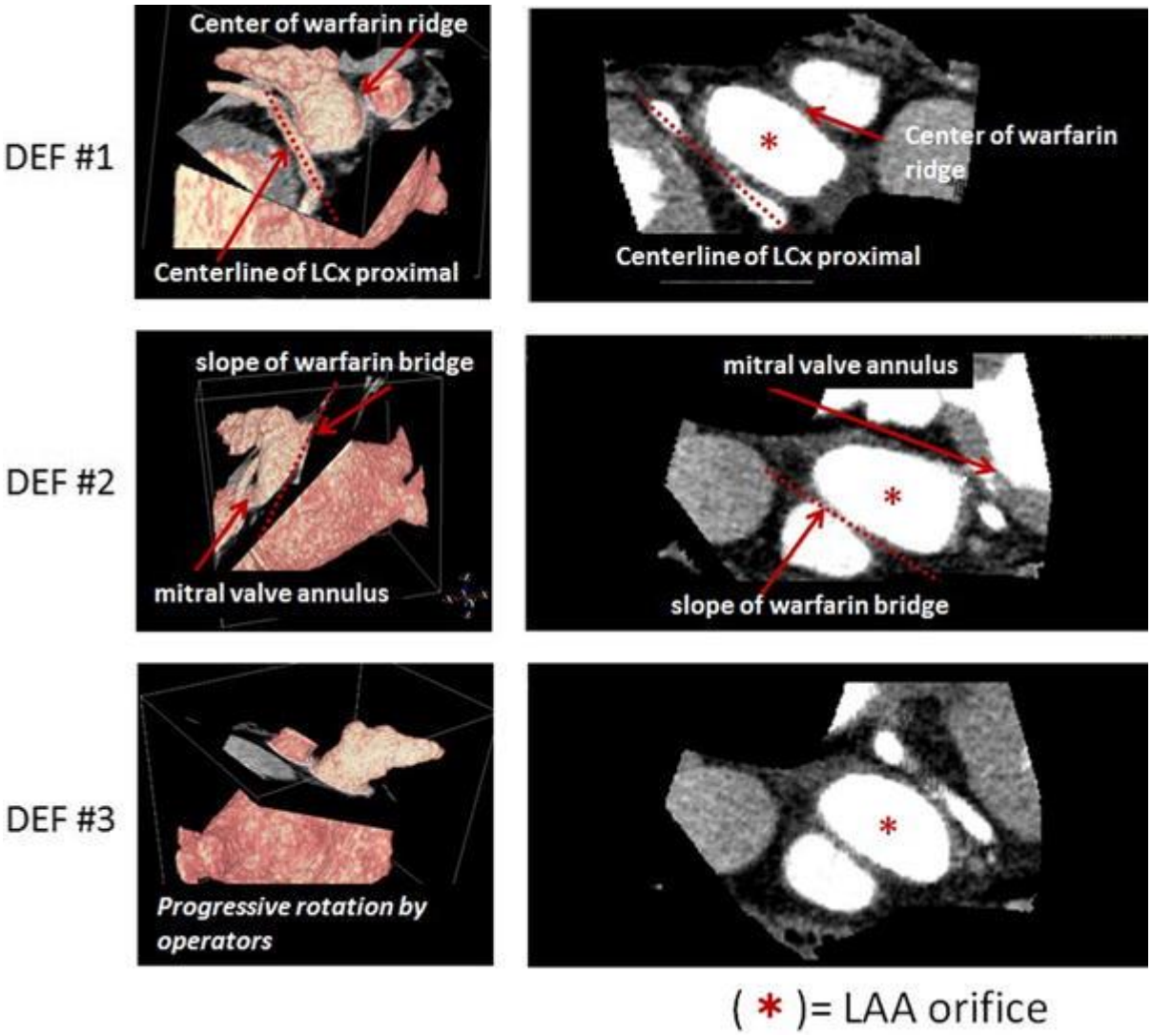

Statistical analyses

All statistical analyses were performed with JMP version 12.0 for Windows (SAS Institute Inc., Cary, NC, USA). Normally distributed continuous variables are expressed as means ± standard deviations (SD). Non-normally distributed continuous variables are expressed as medians and ranges. Categorical variables are expressed as numbers and percentages. Fisher's exact test or paired *t* tests were performed for comparisons. The correlations between each definition were investigated using Bland–Altman plots and a simple linear regression analysis. A P value < 0.05 was considered to denote a statistically significant difference. The inter-observer agreement between observers was evaluated using Spearman's rank-order correlation. A good level of agreement was defined as ρ score > 0.648 ($P < 0.05$).

Results

Baseline clinical characteristics

Baseline clinical characteristics are summarized in Table 1. There were no differences in age and sex between the NSR group and the PAF group. Body mass index was significantly greater in the NSR group than the PAF group, whereas the latter was significantly taller. Atherosclerotic risk factors, including hypertension and dyslipidemia were significantly more frequent in the NSR group than the PAF group. Serum BNP levels in the PAF group were slightly but significantly higher than in the NSR group. On the other hand, no significant differences were observed between the two groups for complications of vascular diseases, including carotid artery aneurysm, coronary artery aneurysm, cerebral aneurysm, and thoracic aortic aneurysm. Importantly, no differences between the two groups were observed in representative parameters of transthoracic echocardiography related to AF, such as left ventricular ejection fraction, left atrial diameter, and prevalence of trace-to-mild mitral regurgitation.

Table 1

Baseline characteristics

	NSR (*n* = 30)	PAF (*n* = 30)	*P* value
Male gender, *n* (%)	21 (70)	23 (76)	0.56
Age (years)	62.3 ± 10.7	63.8 ± 6.0	0.52
Height (cm)	162.0 ± 8.9	167.7 ± 9.0	0.016*
Weight (kg)	64.7 ± 11.6	63.9 ± 10.8	0.78
BMI (kg/m^2)	24.5 ± 3.0	22.6 ± 2.5	0.010*
Hypertension, *n* (%)	19 (63.3)	9 (30)	0.0019*
Diabetes Mellitus, *n* (%)	4 (22.2)	1 (3.3)	0.059
Dyslipidemia, *n* (%)	17 (58.6)	4 (13.3)	0.00040*
Vascular disease, *n* (%)	5 (16.7)	3 (10.0)	0.71
Creatinin (mg/dl)	0.77 ± 0.18	0.80 ± 0.17	0.55
eGFR (ml/min)	80.6 ± 19.6	71.7 ± 13.0	0.044*
BNP (pg/ml)	19.6 ± 9.5	92.4 ± 91.2	0.032*
LVEF (bp-sim) (%)	70.0 ± 4.9	67.6 ± 5.4	0.12
LAD (mm)	38.3 ± 5.4	40.0 ± 6.7	0.36
Mitral regurgitation, *n* (< mild) (%)	17 (89.5)	22 (73.3)	0.28

BMI body mass index, *eGFR* estimated glomerular filtration rate, *BNP* brain natriuretic peptide, *LVEF* left ventricle ejection fraction, *LAD* left atrial dimension

Comparison of LAA parameters between NSR and PAF

Three-dimensional LAA images were successfully reconstructed using our methods for all cases (n = 60). Furthermore, quantitative assessment of LAA dimensions could be performed for all cases without difficulty. Table 2 depicts a comparison of two-dimensional measurements of the LAA orifice plane between the two groups for each of the three definitions. Slight tendencies towards larger areas and greater minimum diameters of the LAA orifice were observed in the PAF group relative to the NSR group according to DEF#1 and #3, but these differences did not achieve statistical significance. Symmetry of the LAA orifice ranged between 0.50 and 0.57, suggesting an elliptical shape.

Table 2

Comparison of two-dimensional measurements of LAA orifice between NSR and PAF patients according to three definitions

LAA orifice	DEF#1			DEF#2			DEF#3		
	NSR (n = 30)	PAF (n = 30)	P value	NSR (n = 30)	PAF (n = 30)	P value	NSR (n = 30)	PAF (n = 30)	P value
Maximum diameter (D), mm	29.8 ± 4.65	31.4 ± 4.92	0.21	33.8 ± 5.39	38.0 ± 5.14	0.0033*	30.6 ± 5.03	31.7 ± 5.57	0.42
Minimum diameter (d), mm	14.9 ± 3.20	16.4 ± 3.60	0.086	18.5 ± 4.20	21.1 ± 4.10	0.021*	16.6 ± 3.49	18.0 ± 4.39	0.17
Symmetry (d/D)	0.50 ± 0.09	0.52 ± 0.10	0.52	0.55 ± 0.13	0.54 ± 0.12	0.84	0.54 ± 0.10	0.57 ± 0.08	0.32
Area (mm^2)	363.8 ± 124.7	426.6 ± 156.4	0.091	493.4 ± 162.1	627.2 ± 191.0	0.0048*	399.7 ± 136.8	458.5 ± 188.3	0.17

Figure 3 illustrates a comparison of LAA volume and LAA volume index between the two groups for the three definitions. In contrast to the 2D assessments of orifice plane, LAA volume of the PAF groups was significantly greater than the NSR group for all 3 definitions (DEF#1: 1.43 times greater, DEF#2: 1.44 times greater, and DEF#3: 1.36 times greater). Furthermore, the LAA volume index, adjusted by BMI, also exhibited consistent differences between the two groups for all three definitions.

Fig. 3

Comparison of LAA volume and LAA volume index between NSR and PAF according to each definition

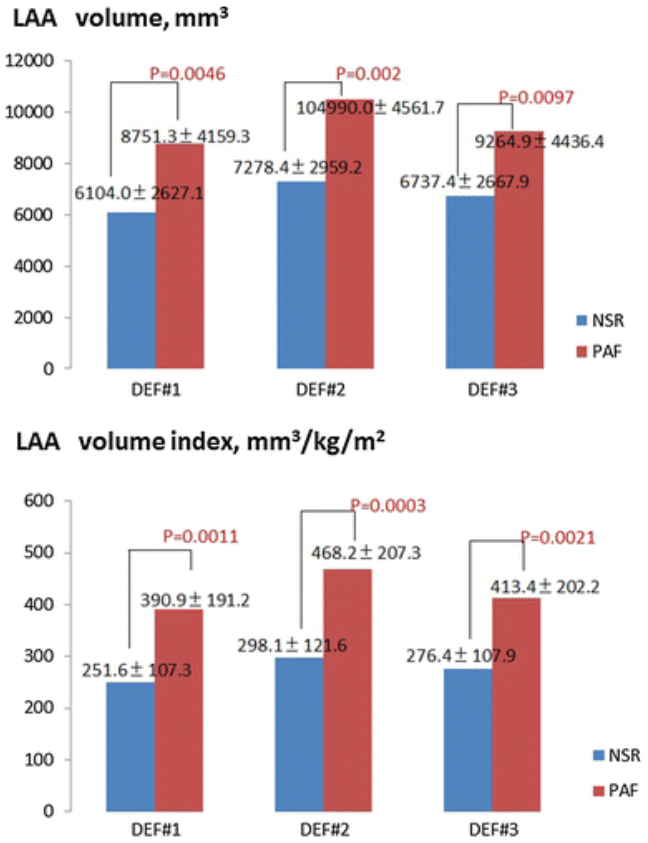

Intra- and inter-observer variability

Intra-observer and inter-observer differences in measurements of the representative LAA parameters were assessed. A total of 10 randomly selected cases was measured repeatedly by one physician (MH) or by two independent expert physicians (MH and KN) according to DEF#1 and then compared. Table 3 clearly indicates that 3D-CT-based quantitative assessment of the LAA provides very reproducible results with little intra-individual and inter-observer variability.

Table 3

Intra-observer and inter-observer differences in measurements

	Intra-observer difference		Inter-observer difference	
	ρ	*P* value	ρ	*P* value
Maximum diameter (*D*), mm	0.76	0.0059*	0.63	0.037*
Minimum diameter (*d*), mm	0.95	< 0.0001*	0.91	0.0001*
Area (mm^2)	0.86	< 0.0006*	0.62	0.043*
Volume (mm^3)	0.95	< 0.0001*	0.92	< 0.0001*

Spearman's rank correlation coefficient: $-1 < \rho < 1$

Discussion

The results of this study can be summarized as follows: (1) LAA volume as well as LAA volume adjusted by BMI was significantly greater in the PAF group compared with the NSR group regardless of which definition of the orifice plane was employed (approximately 1.4 times greater); (2) LAA orifice area was significantly larger in the PAF group than the NSR group according to DEF#2, whereas it tended to be similar by DEF#1 and DEF#3; (3) no difference was observed in orifice symmetry between the two groups, and their oblate ellipses were approximately 50%; (4) our methods for 3D-reconstruction and measurements of the LAA by 3D-CT are feasible and reproducible.

Comparison of LAA sizes between NSR and PAF

Historically, several investigations have demonstrated statistically significant differences in LAA sizes in the three cardiac rhythm groups, NSR, PAF and chronic AF [121314]. Especially, the size of the LAA in patients with chronic AF is greater than in subjects with NSR [514]. However, in terms of "direct comparisons" between PAF and NSR, to date, very few investigations have been published, and they did not show any differences between NSR and PAF [56]. In contrast, the present study did detect differences in volume, considered to be due to the higher spatial resolution and finer quantitative performance of 3D-CT relative to conventional TEE for the visualization of the LAA.

Why is the LAA volume of PAF patients greater than in NSR? Basically, the LAA assists with the adjustability of LA pressure because of its higher compliance compared with the LA wall [15]. Consistent with this, a strong positive correlation was observed between the LAA area and the mean pulmonary capillary wedge pressure [16]. Once patients with heart failure are treated, the degree of reduction of LAA volume is significantly greater than the reduction of LA body volume in that patient [15]. Considering the frequent exposure to elevated LA pressure during PAF, the size of the LAA may increase at a relatively early stage of AF, during PAF.

Impact of the definition of the orifice plane on LAA measurement

Regardless of the definitions of the orifice, the LAA volume of the PAF group was consistently greater than in the NSR subjects. However, two-dimensional assessments of LAA orifice varied according to the definition of orifice plane. Basically, the LAA varies in shape significantly [1718]. This exacerbates the ambiguity of LAA orifice assessments. Accurate measurement of the diameter of the LAA orifice is considered difficult [19], because of lack of a definitive boundary line between the LAA and LA body [8]. Embryologically, the LAA is derived from the atrial primitive, whose luminal surface possesses irregular pectinate muscle that can be discriminated from the smooth surface of the LA body [20]. However, the distribution of this trabeculated portion varies between patients, independent of the structural border between the LA body and the LAA. Accordingly, other obvious landmarks are required to determine the LAA orifice plane, to maintain reproducibility of LAA size measurement. Historically, LAA evaluations have mostly been by TEE. No definitive boundary line exists between the LAA and LA and no definitions have been available for CT-based LAA assessment. Accordingly, we had to define several candidates for the orifice place at the beginning of this investigation. Potential anatomical landmarks for determination of the LAA orifice by CT images include the warfarin ridge, left circumflex coronary artery, and mitral valve annulus, which had also been used in previous TEE studies as established methods [1011]. The present study constructed three useful practical definitions

for 3D-CT evaluation by combining these potential landmarks, which should pose potential systemic biases. Accordingly, Bland–Altman analyses were performed for orifice area and volume to assess systematic errors inherent in the adopted definitions of the LAA orifice plane (Fig. 4). We found that DEF#2, defining the orifice plane by the mitral annulus (line) and slope of the warfarin ridge, had constantly greater values compared with those of the other two definitions. This property needs to be recognized. According to our assessment, we believe DEF#1 and DEF#3 are superior to DEF#2. Of these, DEF#3, the operator's discretion technique, is likely to be affected by operator bias, which would require mature skill sets to maximize reproducibility of selection of the optimal plane.

Fig. 4

Bland–Altman plots to compare orifice area and volume of the LAA for the three definitions of the orifice plane. LAA orifice area and volume tend to be the greatest if we measure by DEF#2. Systemic biases appeared smaller between DEF#1 and DEF#3

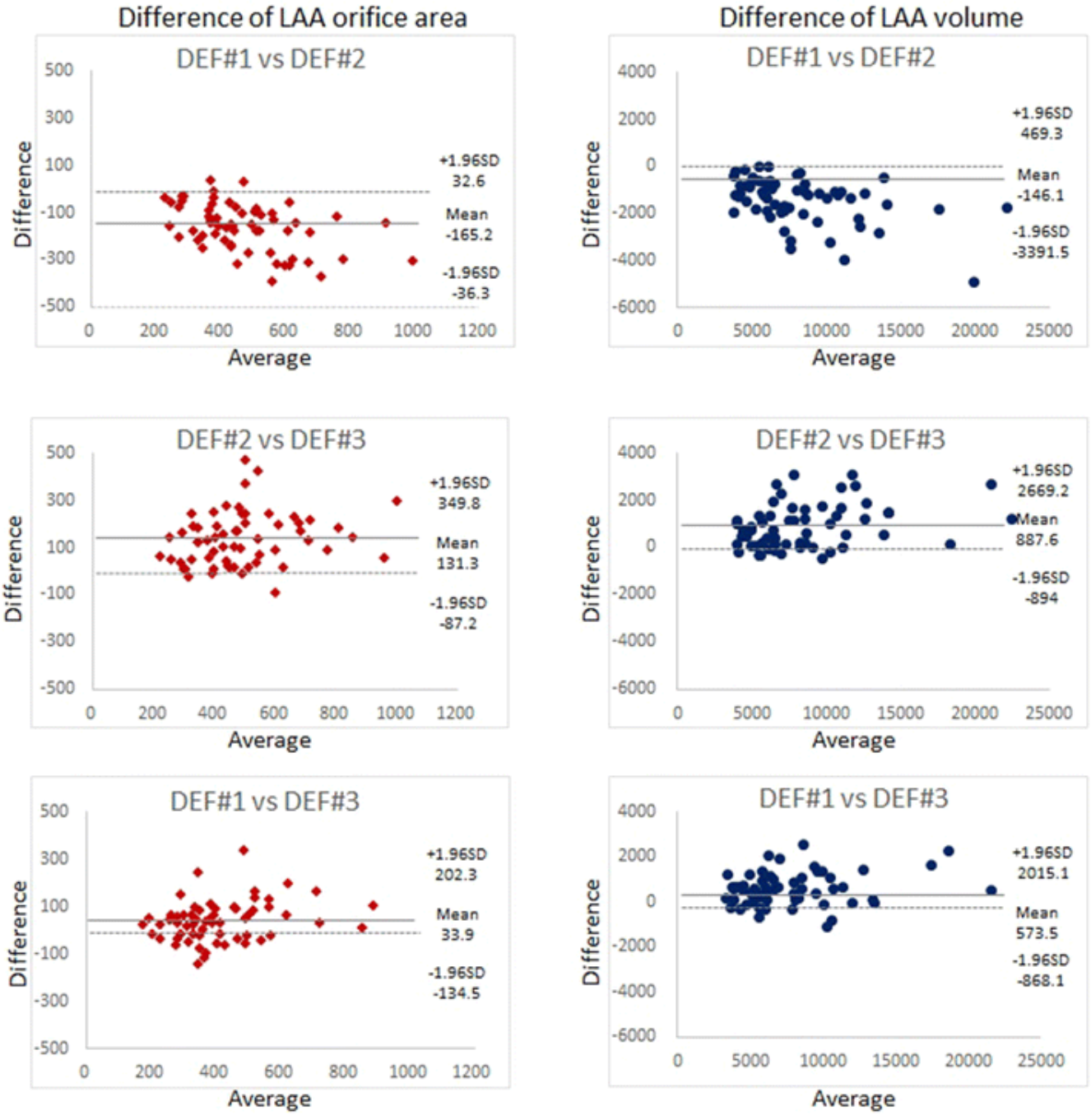

Clinical implications

This study has several evident clinical implications for the assessment of the LAA in terms of risk stratification and medical treatment; differences in the size of the LAA between NSR and PAF have been demonstrated for the first time, motivating a precise evaluation of the LAA even at the paroxysmal stage of atrial arrhythmia. Thus, LAA size significantly correlates with the risk of embolic stroke [421]. Furthermore, the shape of the LAA is also significantly associated with thrombus formation within it [17]. Cardiac CT is the most suitable method for in-depth and accurate assessment of the LAA regarding shape and size, the characteristics of which are significantly associated with the risk of cardiogenic emboli. Our established methods should provide simple and rapid 3D-reconstruction and measurement to satisfy these clinical needs.

The LAA is an important interventional target for stroke prevention with the use of percutaneous closure devices. To avoid serious complications such as cardiac tamponade, procedure-related stroke, device embolism, peri-device leakage, and thrombus embolism related to catheter manipulation [222324], accurate measurement and assessment of the LAA orifice and LAA depth is critically important. Although the implantation of LAA occlusion devices is performed under angiographic and TEE guidance, 3D-CT allows us to understand the anatomical information regarding the location of the LAA relative to the surrounding structures. Moreover, many parameters of the arbitrary plane can be measured, which should be useful for pre-operative treatment planning. Furthermore, the custom software package used in this study facilitates 3D image reconstruction capability, which allows output of actual 3D-model printing quite readily (Fig. 5). Creating life-size 3D-models will be useful for understanding the actual anatomy, especially for the most variable shapes in human beings and for simulating LAA occlusion device implantation [2526].

Fig. 5

Representation of four examples of life-size 3D-printing models of the LAA using the default function of the software package

Limitations

This study has some potential limitations. First, sample size was relatively small. Second, several potential selection biases may have influenced the results; thus, coronary CT images were exclusively used in the NSR group, and as a result, atherosclerotic risk factors including hypertension, diabetes, and dyslipidemia were significantly more frequently observed in this group. To minimize such bias, we calculated adjusted size parameters by BMI. Interestingly, these relationships were maintained when LAA sizes were adjusted by BMI. However, considering the invasiveness of using contrast agents, and the radiation exposure, it is very difficult to perform CT evaluation targeting LAA for NSR subjects for ethical reasons. Furthermore, LAA volumes increase with age regardless of the presence of AF [2728]. However, this bias did not impact on the results obtained, showing greater dimensions of LAA in the PAF group, even considering the higher ages of subjects in the NSR group. Third, the CT protocol was not based on detection at the end-systolic state of the R–R interval of 40% indicating maximum LAA volume [29]. Basically, the LAA contracts and dilates during the cardiac cycle [629]. In fact, we used the end-diastolic phase of the R–R interval of 75% for this study, which potentially did not reflect the maximum volume of LAA. However, the identical cardiac phase was used for both groups, which should allow their comparison. Fourth, patients might undergo CT under dehydrated conditions due to the mandated request of nothing by mouth prior to examination. Because LAA sizes are influenced by intravascular fluid volumes, their absolute volumes and areas may be affected to some extent [30]. Fifth, DEF#3 is very subjective because of progressive rotation based on the observer's visual assessment. However, previous reports have mainly applied this method [12], making it the one available "confirmed" method. Sixth, no investigations were performed regarding the morphology of the LAA, such as chicken wing-type, windsock-type or cactus-type. Fukushima et al. showed that the windsock-type LAA in PAF patients is significantly more frequent than other types [31]. Further studies focusing on the morphological subtypes will be required to determine whether this is an important factor. Finally, the LAA of PAF patients was investigated during their sinus rhythm. Further enlargement as well as reduction of the ejection fraction could be estimated during a PAF attack, so their actual magnitudes remain unknown.

Conclusions

Three-dimensional CT-based quantitative assessment of LAA provides highly reproducible and detailed measurements, which can successfully discriminate differences of LAA volume between patients with NSR and PAF, suggesting that volumes are significantly greater in the latter. The absolute differences in size appear to be relatively small, but these novel findings are considered likely to be of value for developing comprehensive strategies for prevention of cardioembolic stroke.

Acknowledgements

The authors would like to thank Tadashi Sasaki, Kota Takeda, Takuya Chiba, Yuta Ueyama, Akinobu Sasaki, Kei Kikuchi, Takanori Ueda (radiation technologists of Iwate Medical University), Toru Kato, Hiroki Takahashi (graduate students of Iwate Prefectural University) for collecting data and coaching of image-editing in this study.

Compliance with ethical standards

Conflict of interest

The authors declare that they have no conflict of interest.

Ethical standards

This study is a retrospective study. For this type of study formal consent is not required.

References

1. Disertori M, Franzosi MG, Barlera S, Cosmi F, Quintarelli S, Favero C, Cappellini G, Fabbri G, Maggioni AP, Staszewsky L, Moroni LA, Latini R, Investigators G-A (2013) Thromboembolic event rate in paroxysmal and persistent atrial fibrillation: data from the GISSI-AF trial. BMC Cardiovasc Disord 13:28
2. Agmon Y, Khandheria BK, Gentile F, Seward JB (1999) Echocardiographic assessment of the left atrial appendage. J Am Coll Cardiol 34:1867–1877
3. Narumiya T, Sakamaki T, Sato Y, Kanmatsuse K (2003) Relationship between left atrial appendage function and left atrial thrombus in patients with nonvalvular chronic atrial fibrillation and atrial flutter. Circ J 67:68–72
4. Burrell LD, Horne BD, Anderson JL, Muhlestein JB, Whisenant BK (2013) Usefulness of left atrial appendage volume as a predictor of embolic stroke in patients with atrial fibrillation. Am J Cardiol 112:1148–1152
5. Nucifora G, Faletra FF, Regoli F, Pasotti E, Pedrazzini G, Moccetti T, Auricchio A (2011) Evaluation of the left atrial appendage with real-time 3-dimensional transesophageal echocardiography: implications for catheter-based left atrial appendage closure. Circ Cardiovasc Imaging 4:514–523
6. Matsumoto Y, Morino Y, Kumagai A, Hozawa M, Nakamura M, Terayama Y, Tashiro A (2017) Characteristics of anatomy and function of the left atrial appendage and their relationships in patients with cardioembolic stroke: a 3-dimensional transesophageal echocardiography study. J Stroke Cerebrovasc Dis 26:470–479
7. Doi A, Takahashi H, Syuto B, Katayama M, Nagashima H, Okumura M (2013) Tailor-made plate design and manufacturing system for treating bone fractures in small animals. J Adv Comput Intell Intell Inform 17:1–10
8. Budge LP, Shaffer KM, Moorman JR, Lake DE, Ferguson JD, Mangrum JM (2008) Analysis of in vivo left atrial appendage morphology in patients with atrial fibrillation: a direct comparison of transesophageal echocardiography, planar cardiac CT, and segmented three-dimensional cardiac CT. J Interv Card Electrophysiol 23:87–93
9. Yosefy C, Laish-Farkash A, Azhibekov Y, Khalameizer V, Brodkin B, Katz A (2016) A new method for direct three-dimensional measurement of left atrial appendage dimensions during transesophageal echocardiography. Echocardiography 33:69–76
10. Mobius-Winkler S, Sandri M, Mangner N, Lurz P, Dahnert I, Schuler G (2012) The WATCHMAN left atrial appendage closure device for atrial fibrillation. J Vis Exp 60:3671
11. Masoudi FA, Calkins H, Kavinsky CJ, Drozda JP Jr, Gainsley P, Slotwiner DJ, Turi ZG (2015) 2015 ACC/HRS/SCAI left atrial appendage occlusion device societal overview. J Am Coll Cardiol 66:1497–1513

12. Walker DT, Humphries JA, Phillips KP (2012) Anatomical analysis of the left atrial appendage using segmented, three-dimensional cardiac CT: a comparison of patients with paroxysmal and persistent forms of atrial fibrillation. J Interv Card Electrophysiol 34:173–179
13. Imada M, Funabashi N, Asano M, Uehara M, Ueda M, Komuro I (2007) Anatomical remodeling of left atria in subjects with chronic and paroxysmal atrial fibrillation evaluated by multislice computed tomography. Int J Cardiol 119:384–388
14. Lacomis JM, Goitein O, Deible C, Moran PL, Mamone G, Madan S, Schwartzman D (2007) Dynamic multidimensional imaging of the human left atrial appendage. Europace 9:1134–1140
15. Ito T, Suwa M, Kobashi A, Yagi H, Hirota Y, Kawamura K (1998) Influence of altered loading conditions on left atrial appendage function in vivo. Am J Cardiol 81:1056–1059
16. Tabata T, Oki T, Yamada H, Abe M, Onose Y, Thomas JD (2000) Relationship between left atrial appendage function and plasma concentration of atrial natriuretic peptide. Eur J Echocardiogr 1:130–137
17. Di Biase L, Santangeli P, Anselmino M, Mohanty P, Salvetti I, Gili S, Horton R, Sanchez JE, Bai R, Mohanty S, Pump A, Cereceda Brantes M, Gallinghouse GJ, Burkhardt JD, Cesarani F, Scaglione M, Natale A, Gaita F (2012) Does the left atrial appendage morphology correlate with the risk of stroke in patients with atrial fibrillation? Results from a multicenter study. J Am Coll Cardiol 60:531–538
18. Beutler DS, Gerkin RD, Loli AI (2014) The morphology of left atrial appendage lobes: a novel characteristic naming scheme derived through three-dimensional cardiac computed tomography. World J Cardiovasc Surg 4:17–24
19. Wang Y, Di Biase L, Horton RP, Nguyen T, Morhanty P, Natale A (2010) Left atrial appendage studied by computed tomography to help planning for appendage closure device placement. J Cardiovasc Electrophysiol 21:973–982
20. Abdulla R, Blew GA, Holterman MJ (2004) Cardiovascular embryology. Pediatr Cardiol 25:191–200
21. Taina M, Vanninen R, Hedman M, Jakala P, Karkkainen S, Tapiola T, Sipola P (2013) Left atrial appendage volume increased in more than half of patients with cryptogenic stroke. PLoS One 8:e79519
22. Chung H, Jeon B, Chang HJ, Han D, Shim H, Cho IJ, Shim CY, Hong GR, Kim JS, Jang Y, Chung N (2015) Predicting peri-device leakage of left atrial appendage device closure using novel three-dimensional geometric CT analysis. J Cardiovasc Ultrasound 23:211–218
23. Holmes DR, Reddy VY, Turi ZG, Doshi SK, Sievert H, Buchbinder M, Mullin CM, Sick P, Investigators PA (2009) Percutaneous closure of the left atrial appendage versus warfarin therapy for prevention of stroke in patients with atrial fibrillation: a randomised non-inferiority trial. Lancet 374:534–542
24. Reddy VY, Doshi SK, Sievert H, Buchbinder M, Neuzil P, Huber K, Halperin JL, Holmes D, Investigators PA (2013) Percutaneous left atrial appendage closure for stroke prophylaxis in patients with atrial fibrillation: 2.3-Year Follow-up of the PROTECT AF (Watchman Left Atrial Appendage System for Embolic Protection in Patients with Atrial Fibrillation) Trial. Circulation 127:720–729
25. Otton JM, Spina R, Sulas R, Subbiah RN, Jacobs N, Muller DW, Gunalingam B (2015) Left atrial appendage closure guided by personalized 3D-printed cardiac reconstruction. JACC Cardiovasc Interv 8:1004–1006

26. Pracon R, Grygoruk R, Dzielinska Z, Kepka C, Dabrowska A, Konka M, Jazwiec P, Reczuch K, Witkowski A, Demkow M (2016) Percutaneous occlusion of the left atrial appendage with complex anatomy facilitated with 3D-printed model of the heart. EuroIntervention 12:927
27. Boucebci S, Pambrun T, Velasco S, Duboe PO, Ingrand P, Tasu JP (2016) Assessment of normal left atrial appendage anatomy and function over gender and ages by dynamic cardiac CT. Eur Radiol 26:1512–1520
28. Veinot JP, Harrity PJ, Gentile F, Khandheria BK, Bailey KR, Eickholt JT, Seward JB, Tajik AJ, Edwards WD (1997) Anatomy of the normal left atrial appendage: a quantitative study of age-related changes in 500 autopsy hearts: implications for echocardiographic examination. Circulation 96:3112–3115
29. Erol B, Karcaaltincaba M, Aytemir K, Cay N, Hazirolan T, Akata D (2011) Analysis of left atrial appendix by dual-source CT coronary angiography: morphologic classification and imaging by volume rendered CT images. Eur J Radiol 80:e346–e350
30. Spencer RJ, DeJong P, Fahmy P, Lempereur M, Tsang MY, Gin KG, Lee PK, Nair P, Tsang TS, Jue J, Saw J (2015) Changes in left atrial appendage dimensions following volume loading during percutaneous left atrial appendage closure. JACC Cardiovasc Interv 8:1935–1941
31. Fukushima K, Fukushima N, Kato K, Ejima K, Sato H, Fukushima K, Saito C, Hayashi K, Arai K, Manaka T, Ashihara K, Shoda M, Hagiwara N (2016) Correlation between left atrial appendage morphology and flow velocity in patients with paroxysmal atrial fibrillation. Eur Heart J Cardiovasc Imaging 17:59–66